Published in final edited form as:
Sci Signal. ; 3(141): ra70. doi:10.1126/scisignal.2001152.

Molecular Mechanism of Calcium Channel Regulation in the Fight-or-Flight Response

Matthew D. Fuller[1], **Michelle A. Emrick**[1,*], **Martin Sadilek**[2], **Todd Scheuer**[1], and **William A. Catterall**[1,†]

[1] Department of Pharmacology, University of Washington, Box 357280, Seattle, WA 98195-7280, USA

[2] Department of Chemistry, Box 351700, University of Washington, Seattle, WA 98195-1700, USA

Abstract

During the fight-or-flight response, the sympathetic nervous system stimulates L-type calcium ion (Ca^{2+}) currents conducted by Ca_V1 channels through activation of β-adrenergic receptors, adenylyl cyclase, and phosphorylation by adenosine 3′,5′-monophosphate–dependent protein kinase [also known as protein kinase A (PKA)], increasing contractility of skeletal and cardiac muscles. We reconstituted this regulation of cardiac $Ca_V1.2$ channels in non-muscle cells by forming an autoinhibitory signaling complex composed of $Ca_V1.2\Delta1800$ (a form of the channel truncated at the in vivo site of proteolytic processing), its noncovalently associated distal carboxyl-terminal domain, the auxiliary $\alpha_2\delta_1$ and β_{2b} subunits, and A-kinase anchoring protein 15 (AKAP15). A factor of 3.6 range of $Ca_V1.2$ channel activity was observed from a minimum in the presence of protein kinase inhibitors to a maximum upon activation of adenylyl cyclase. Basal $Ca_V1.2$ channel activity in unstimulated cells was regulated by phosphorylation of serine-1700 and threonine-1704, two residues located at the interface between the distal and the proximal carboxyl-terminal regulatory domains, whereas further stimulation of channel activity through the PKA signaling pathway only required phosphorylation of serine-1700. Our results define a conceptual framework for $Ca_V1.2$ channel regulation and identify sites of phosphorylation that regulate channel activity.

INTRODUCTION

The “fight-or-flight” response is a conserved behavior of vertebrates experiencing fear, stress, or intense exercise. Release of epinephrine from the adrenal medulla and norepinephrine from sympathetic nerve endings activates β-adrenergic receptors and leads to an increase in L-type Ca^{2+} currents in cardiac and skeletal muscle, which in turn increase the

†To whom correspondence should be addressed. wcatt@u.washington.edu.
*Present address: VLST Corporation, 307 Westlake Avenue North, Seattle, WA 98109, USA.

SUPPLEMENTARY MATERIALS
www.sciencesignaling.org/cgi/content/full/3/141/ra70/DC1
Fig. S1. Inhibition of $Ca_V1.2\Delta1800$ channels by DCT.
Fig. S2. Modulation of $Ca_V1.2$ channel activity in single cells requires coexpression of AKAP15.
Fig. S3. Alanine substitutions have no effect on $Ca_V1.2\Delta1800$ channel activity in the absence of DCT.
Materials and Methods
References

Author contributions: W.A.C., T.S., M.D.F., and M.A.E. conceived the research. M.D.F., M.A.E., M.S., T.S., and W.A.C. designed and performed the experiments and analyzed the data. W.A.C., M.D.F., M.A.E., and T.S. wrote the paper.

Competing interests: The authors declare that they have no competing interests.

force of contraction of skeletal muscle and the beating rate and contractility of the heart (1–3). This regulation of L-type calcium currents occurs through activation of protein kinase A (PKA)–mediated phosphorylation (4–8), but the molecular mechanism is unknown.

$Ca_V1.1$ and $Ca_V1.2$ channels, which conduct L-type Ca^{2+} currents in skeletal and cardiac muscle, respectively, are composed of pore-forming α_1 subunits, plus auxiliary $\alpha_2\delta$ and β subunits (9–17). The α_1 subunits of $Ca_V1.1$ and $Ca_V1.2$ channels each exist as two size forms produced by in vivo proteolytic processing of the C terminus in skeletal and cardiac muscle (18–22) and in brain (23,24). Expression of complementary DNA (cDNA) encoding full-length $Ca_V1.2$ channels in non-muscle cells yields only full-length α_1 subunits with no evidence of proteolytic processing (25). Deletion of the distal C terminus increases $Ca_V1.2$ channel activity (26,27), and coexpression of the distal C terminus results in formation of a noncovalent autoinhibitory complex with the proximal C terminus of the truncated channel (28). The distal C-terminal domain effectively inhibits Ba^{2+} currents and reduces coupling efficiency between voltage sensor movement and opening of the pore (21,28).

Ca_V1 channels in skeletal and cardiac muscle bind A-kinase anchoring protein 15 (AKAP15) (29–31), and β-adrenergic regulation of these channels requires PKA anchored by AKAP15 (32,33). The AKAP15-PKA complex interacts with a site located in the proteolytically cleaved distal C terminus, suggesting that the distal C terminus remains associated with the remainder of the channel and mediates PKA-dependent regulation in cardiac myocytes (28,33,34).

Physiological regulation of L-type currents by PKA has not been reconstituted in non-muscle cells, impeding detailed analysis of the regulatory properties of calcium channel mutants. Previous studies of PKA-dependent modulation of cloned $Ca_V1.2$ channels expressed in non-muscle cells have examined full-length channels [for instance, (35,36)]. Here we show that PKA-dependent modulation of $Ca_V1.2$ channel activity with a dynamic range similar to that seen in cardiac myocytes can be reconstituted in non-muscle cells after optimized expression of the different components of the $Ca_V1.2$-AKAP15 autoinhibitory signaling complex. Using this reconstitution system, we have identified sites of protein phosphorylation that are both necessary and sufficient for physiological regulation of $Ca_V1.2$ channels in non-muscle cells. These sites are located at the interface between the proximal (PCRD) and the distal (DCRD) C-terminal regulatory domains, well positioned to mediate disinhibition of the auto-inhibitory signaling complex and increase $Ca_V1.2$ channel activity in the fight-or-flight response.

RESULTS

Reconstitution of an autoinhibitory $Ca_V1.2$ channel signaling complex

The distal C-terminal domain inhibits channel activity when cDNA encoding $distal_{1822–2171}$ is coexpressed at a 5:1 molar ratio with that encoding $Ca_V1.2$ channels truncated at position 1821 (28). For the experiments described here, we cotransfected cDNA encoding $Ca_V1.2$ channels truncated at A^{1800}, the exact site of in vivo proteolytic processing ($Ca_V1.2\Delta1800$) (21), $distal_{1801–2171}$ (DCT), $\alpha_2\delta_1$, and β_{1b} to produce a functional auto-inhibitory $Ca_V1.2$ channel complex. We assessed channel activity by measuring peak Ba^{2+} current and by determining the coupling efficiency of pore opening to gating charge movement (28). Gating charge movement was measured by integrating the gating current during depolarization to the reversal potential, and pore opening was measured from tail currents upon repolarization from the reversal potential. The functional properties of $Ca_V1.2\Delta1800$ channels and their inhibition by DCT were identical to those of $Ca_V1.2\Delta1821$ and $distal_{1822–2171}$ [compare (28) and fig. S1].

Transfection of cells with increasing ratios of cDNA encoding DCT to cDNA encoding $Ca_V1.2\Delta1800$ revealed increasing inhibition of channel activity, with maximal inhibition at a ratio of 0.75 (Fig. 1, A and B). Coexpression of the DCT with the truncated channel does not alter the density of $Ca_V1.2$ channels on the cell surface, as determined by gating current measurements (28); therefore, reduction of the tail current provides a direct measure of the decrease in the coupling efficiency of the gating charge movement to opening of the pore: 43.6 ± 2.4 nA/pC (n = 13) for $Ca_V1.2\Delta1800$ channels versus 15.2 ± 1.0 nA/pC for $Ca_V1.2\Delta1800$ + DCT (n = 19; $P < 0.01$) (Fig. 1A).

Inward Ba^{2+} currents conducted by $Ca_V1.2$ channels were decreased when DCT was present, similar to previous results (Fig. 1C) (28). However, the shift in voltage-dependent activation to more depolarizing potentials observed with large amounts of $distal_{1822–2171}$ (28) was barely detectable (but still significant) with smaller amounts of DCT (Fig. 1D). These results suggest that expression of an optimal 0.75:1 molar ratio of the cDNAs encoding DCT and $Ca_V1.2\Delta1800$ causes a specific reduction in coupling efficiency of gating charge movement to pore opening.

Reduction of basal $Ca_V1.2$ channel activity by inhibition of protein kinases

The increase in L-type Ca^{2+} current caused by basal phosphorylation in unstimulated cardiac myocytes (37) is inhibited by 1 μM RO 31-8220 (38), a potent protein kinase C (PKC) inhibitor (39) that also inhibits PKA and other protein kinases at 1 μM and higher concentrations (40). To determine whether protein kinase inhibition would also decrease L-type current through $Ca_V1.2$ channels in tsA-201 human embryonic kidney cells, we applied RO 31-8220 (50 nM or 1 μM) to the extracellular surface of cells transiently transfected with cDNAs encoding $Ca_V1.2\Delta1800$ + DCT for 5 min before recording channel activity. RO 31-8220 (1 μM) significantly decreased inward Ba^{2+} currents and coupling efficiency in cells expressing $Ca_V1.2\Delta1800$ + DCT (Fig. 2, brown). In contrast, 50 nM RO 31-8220, an effective concentration for inhibiting PKC but not PKA (40), had no effect on channel activity. We also observed a significant decrease in basal channel activity when cells expressing $Ca_V1.2\Delta1800$ + DCT were treated for 1 hour with the specific, membrane-permeant PKA inhibitor myristoylated PKI 14-22 amide (5 μM) before recording channel activity with an intracellular solution containing 2 μM PKI 6-22 amide, the same PKA inhibitor in membrane-impermeant form (Fig. 2, C and D). Collectively, these results indicate that PKA-dependent phosphorylation increases basal $Ca_V1.2$ channel activity. The coupling efficiency during PKA inhibition defines the lower limit of $Ca_V1.2$ channel activity compared to the maximal coupling efficiency for $Ca_V1.2\Delta1800$ channels in the absence of DCT.

Requirement for AKAP15 for PKA-dependent increase in $Ca_V1.2$ channel activity

AKAPs act as molecular scaffolds that enable the formation of signaling complexes (41). AKAP15 directly associates with $Ca_V1.1$ and $Ca_V1.2$ channels through a modified leucine zipper motif and promotes their co-localization with PKA (29–33). Moreover, physiological regulation of $Ca_V1.2$ channels by β-adrenergic stimulation in dissociated cardiac myocytes requires PKA anchored to AKAP15 (33). To test the requirement for AKAP15, we applied 5 μM forskolin to cells transfected with cDNA encoding $Ca_V1.2\Delta1800$ + DCT for 5 min before recording channel activity. No increase in coupling efficiency was observed in the absence of AKAP15 (Fig. 3A). However, titration of the cDNA encoding AKAP15 downward from a molar ratio of 1:1 relative to that encoding $Ca_V1.2\Delta1800$ revealed a substantial increase in coupling efficiency by forskolin at low amounts of AKAP15 (Fig. 3A, blue). With the optimum amount of AKAP15, forskolin increased $Ca_V1.2\Delta1800$ + DCT coupling efficiency to 28.0 ± 2.0 nA/pC versus 15.2 ± 1.0 nA/pC for control without forskolin (n = 19 to 20, $P < 0.01$), with a corresponding increase in inward Ba^{2+} current

(Fig. 3C), suggesting that AKAP15 is required for PKA-dependent $Ca_V1.2$ channel regulation. Comparison of the results with forskolin treatment (Fig. 3) to the results with kinase inhibitors (Fig. 2) revealed a factor of 3.6 dynamic range of modulation of $Ca_V1.2$ channel activity, similar to that seen in dissociated cardiac myocytes (25,34,38). Acute application of 5 μM forskolin to tsA-201 cells expressing $Ca_V1.2\Delta1800$ + DCT with the optimum amount of AKAP15 gave a similar dynamic range of modulation (Fig. 3B). To ensure maximum activation of PKA in an undisturbed cellular context, we performed all subsequent experiments on intact $Ca_V1.2$-expressing cells treated with 5 μM forskolin for 5 min before recording channel activity.

Overexpressed AKAP15 is expected to have a dominant-negative effect on regulation of $Ca_V1.2$ channel activity when its concentration exceeds that of endogenous PKA, so that AKAP15 lacking bound PKA occupies the $Ca_V1.2$ channel binding sites unproductively. This necessitated the use of low molar ratios of the cDNA encoding AKAP15 to those encoding $Ca_V1.2\Delta1800$ + DCT. Analysis of coupling efficiency in individual cells indicated that 65% of cells cotransfected with AKAP15 and $Ca_V1.2\Delta1800$ + DCT showed higher coupling efficiencies when treated with 5 μM forskolin than the maximum observed in its absence (fig. S2, A and B). In contrast, no individual cells had coupling efficiencies in the same range when $Ca_V1.2\Delta1800$ + DCT channels lacking AKAP15 were treated with 5 μM forskolin (fig. S2A). The mean coupling efficiency in cells responsive to forskolin treatment was 33.5 ± 1.6 nA/pC (n = 13), whereas unresponsive cells had a mean coupling efficiency of 17.9 ± 0.8 nA/pC (n = 7), similar to that observed for $Ca_V1.2\Delta1800$ + DCT in the absence of forskolin (fig. S2C). These findings show that PKA-dependent modulation of $Ca_V1.2$ channel activity can be reconstituted in non-muscle cells, but only in the presence of optimal amounts of AKAP15. To circumvent the dominant-negative effect of AKAP15, we coexpressed cDNA encoding PKA together with those encoding $Ca_V1.2\Delta1800$ + DCT and AKAP15. Under these conditions, each individual cell exhibited a coupling efficiency in the presence of forskolin higher than that seen in its absence (Fig. 3, D and E). These results suggest that PKA overexpression ensures that an AKAP15-PKA complex associates with each $Ca_V1.2\Delta1800$ + DCT channel to mediate forskolin-dependent modulation. However, all subsequent experiments were performed in the absence of exogenous PKA to avoid unwanted effects of kinase overexpression that might result from phosphorylation of secondary sites.

Modulation of full-length $Ca_V1.2$ channels by AKAP15

Earlier attempts to reconstitute PKA-dependent modulation of $Ca_V1.2$ channels in non-muscle cells used full-length channels ($Ca_V1.2$FL) and showed only small increases in $Ca_V1.2$ channel activity in response to PKA activation [for instance, (31,35,36,42)]. To determine whether the effects of PKA on $Ca_V1.2$FL channel activity were enhanced in the presence of optimal amounts of AKAP15, we recorded $Ca_V1.2$FL channel activity in the presence and absence of 5 μM forskolin in cells coexpressing AKAP15. In contrast to $Ca_V1.2\Delta1800$ + DCT, 5 μM forskolin failed to elicit a significant increase in coupling efficiency for $Ca_V1.2$FL at AKAP15 cDNA ratios of 0.003:1 and 1:1 (Fig. 4A, gray and blue), although it produced a small but significant increase in inward Ba^{2+} current (Fig. 4B, blue; 5.0 ± 0.6 nA/pC versus 7.4 ± 0.6 nA/pC, n = 7; $P < 0.05$). Inhibition of protein kinases with 1 μM RO 31-8220 decreased coupling efficiency of $Ca_V1.2$FL from 17.8 ± 1.5 to 7.0 ± 1.0 (Fig. 4A, brown; n = 5; $P < 0.01$) and also decreased Ba^{2+} current (Fig. 4B, brown; n = 5; $P < 0.05$). These results show that regulation of basal activity of $Ca_V1.2$FL is similar or greater than $Ca_V1.2\Delta1800$ + DCT, but up-regulation by PKA is substantially reduced in channels with the distal C terminus covalently attached.

Phosphorylation of sites at the regulatory interface between the distal and the proximal C-terminal domains of $Ca_V1.2$ channels

Successful reconstitution of $Ca_V1.2$ channel modulation provided the opportunity to identify phosphorylation sites that are important for PKA-dependent potentiation of L-type calcium current. Ser^{1928} in the distal C terminus is phosphorylated in response to β-adrenergic stimulation in cardiac myocytes (20,25,43). However, its phosphorylation is not required for the increase in L-type channel activity elicited by β-adrenergic stimulation of cardiac myocytes (34,44). We identified two previously unrecognized phosphorylation sites in the C terminus of the $Ca_V1.1$ channel by mass spectrometry (MS) (45), and these sites are conserved in the $Ca_V1.2$ at Ser^{1700} and Thr^{1704} (Fig. 5A). Ser^{1700} is predicted to be a substrate for PKA and calcium/calmodulin-dependent protein kinase II (CaMKII), whereas Thr^{1704} is predicted to be a substrate of casein kinase II (http://www.phosphosite.org). Both of these sites reside at the interface between the PCRD and the DCRD, where introduction of negatively charged phosphates could disrupt ionic interactions and relieve autoinhibition (Fig. 5A) (28). Analysis of in vitro phosphorylation of glutathione *S*-transferase (GST)–labeled $Ca_V1.2$(1670–1731) by MS showed that Ser^{1700} was a good substrate for both PKA and CaMKII with 27% and 77% phosphorylation, respectively, whereas 10% of Thr^{1704} was phosphorylated by casein kinase II (Fig. 5B). The extents of protein phosphorylation observed in these in vitro experiments reflect both the amino acid sequence contexts of the substrate sites and the local secondary and tertiary structures of the GST-labeled C-terminal protein, which may not retain native conformation in the absence of the complete $Ca_V1.2$ channel and its associated proteins.

We used phosphospecific antibodies and immunocytochemistry to assess PKA phosphorylation of Ser^{1700} and Ser^{1928} in $Ca_V1.2$ channels expressed in tsA-201 cells. Cells expressing $Ca_V1.2\Delta1800$ + DCT were treated with 10 μM forskolin to activate adenylyl cyclase and PKA, or 5 μM ionomycin to increase intracellular Ca^{2+} concentration and thereby activate CaMKII. Cells were fixed and antibody against pS^{1700} immunoreactivity was visualized by indirect immunofluorescence. We observed an increase in phosphorylation of Ser^{1700} after treatment with forskolin or ionomycin in the presence of 1 μM okadaic acid to inhibit phosphoprotein phosphatases 1 and 2A (Fig. 5C). When tested alone, neither okadaic acid (10 nM) nor the calcineurin inhibitor cyclosporin A (10 nM) substantially increased phosphorylation of Ser^{1700} (Fig. 5C). These results indicate that both PKA and CaMKII can phosphorylate Ser^{1700} of $Ca_V1.2$ channels in tsA-201 cells.

Immunoblot analysis showed measurable basal phosphorylation of Ser^{1700} and small increases in antibody against pS^{1700} immunoreactivity when cells expressing $Ca_V1.2\Delta1800$ channels were treated with ionomycin in the presence of okadaic acid or with forskolin in the presence of okadaic acid and cyclosporin A (Fig. 5D). A more substantial increase in phosphorylation at Ser^{1700} was observed for $Ca_V1.2\Delta1800$ + DCT after treatment with forskolin (factor of 1.8 ± 0.4, $P < 0.05$, $n = 3$; Fig. 5D) or ionomycin (factor of 2.5 ± 0.04, $P < 0.01$, $n = 3$; Fig. 5D) in the presence of okadaic acid or cyclosporin A or both. A small increase in phosphorylation was also observed with a phosphospecific antibody directed against Ser^{1928} with both ionomycin and forskolin treatment (Fig. 5D). The Ca^{2+}-dependent increase in phosphorylation of Ser^{1700} was blocked by inhibition of CaMKII with either CaMK inhibitory protein or autocamtide-2–related inhibitor peptide II (1 μM) (Fig. 5E). In contrast to these results with $Ca_V1.2\Delta1800$ + DCT, we observed no change in phosphorylation of Ser^{1700} of $Ca_V1.2$FL channels with drug treatment (forskolin: factor of 0.8 ± 0.1, $P > 0.2$; ionomycin: factor of 1.5 ± 0.7, $P > 0.05$; Fig. 5D). However, we did observe a robust increase in phosphorylation at Ser^{1928} in $Ca_V1.2$FL channels (Fig. 5D). These results demonstrate a difference in PKA phosphorylation of Ser^{1700} between $Ca_V1.2$FL and $Ca_V1.2\Delta1800$ + DCT channels. Evidently, Ser^{1700} is a substrate for basal PKA-dependent phosphorylation of $Ca_V1.2$ channels in transfected cells, but the increase in

PKA phosphorylation of Ser^{1700} is blocked by covalent association of the distal C terminus in $Ca_V1.2$FL.

Phosphorylation sites required for basal $Ca_V1.2$ channel activity

To test the role of individual phosphorylation sites in control of basal $Ca_V1.2$ channel activity, we made alanine substitutions for Ser^{1700}, Thr^{1704}, and Ser^{1928} and recorded channel activity. The S1700A and T1704A mutations had no significant effects on the high activity of $Ca_V1.2\Delta1800$ channels expressed without DCT (fig. S3). However, both S1700A and T1704A significantly reduced the basal coupling efficiency of $Ca_V1.2\Delta1800$ + DCT and decreased basal Ba^{2+} currents (Fig. 6A, gray, blue), whereas S1928A did not have a significant effect (Fig. 6A, orange). The only double-alanine mutation to significantly reduce both basal coupling efficiency and Ba^{2+} currents of $Ca_V1.2\Delta1800$ + DCT was S1700A, T1704A (Fig. 6B, cyan). These results indicate that phosphorylation of Ser^{1700} and Thr^{1704} increases basal activity of $Ca_V1.2\Delta1800$ + DCT channels, whereas phosphorylation of Ser^{1928} does not.

The largest reduction of basal Ba^{2+} currents and coupling efficiency was observed with $Ca_V1.2\Delta1800$ + DCT channels containing alanine substitutions at each phosphorylation site (Fig. 6C, bright green); both the low coupling efficiency and the Ba^{2+} current for the triple-alanine mutant were similar to those observed for wild-type $Ca_V1.2\Delta1800$ + DCT during inhibition of protein kinase activity (Fig. 6C, brown). Analogous results were observed for $Ca_V1.2$FL channels (Fig. 6D). These results show that the basal $Ca_V1.2$ channel activity depends on phosphorylation of Thr^{1704} and Ser^{1700}, but not on phosphorylation of Ser^{1928}.

Phosphorylation sites required for PKA stimulation of $Ca_V1.2$ channel activity

We tested the role of phosphorylation of Ser^{1700}, Thr^{1704}, and Ser^{1928} in PKA-dependent stimulation of $Ca_V1.2$ channels by stimulating adenylyl cyclase with 5 μM forskolin. No forskolin-induced stimulation of the triple-alanine mutant was observed (Fig. 7, A and B, bright green) compared to wild-type channels treated with RO 31-8220 (1 μM) (Fig. 7A, brown). These results indicate that both PKA-stimulated activity and basal activity of $Ca_V1.2$ channels require phosphorylation of one or more of these three sites.

Restoration of Ser^{1928} had no effect (Fig. 7, A and B, cyan). Restoration of Thr^{1704} restored basal channel activity but not forskolin-stimulated activity (Fig. 7, A and B, yellow). Restoration of Ser^{1700} yielded substantial PKA-dependent stimulation of coupling efficiency and Ba^{2+} currents (Fig. 7, A and B, purple), similar to the effects of forskolin on wild-type $Ca_V1.2\Delta1800$ + DCT. Together, these results define distinct roles for phosphorylation of Ser^{1700}, Thr^{1704}, and Ser^{1928} in regulation of $Ca_V1.2$ channels: Phosphorylation of Thr^{1704} contributes primarily to basal regulation of channel function, whereas phosphorylation of Ser^{1700} is uniquely required for PKA-dependent enhancement of channel activity. A similar pattern emerged when $Ca_V1.2$ channels containing only a single-alanine substitution were studied (Fig. 7, A and C). Mutant S1700A lost PKA-dependent modulation of $Ca_V1.2$ channel activity but retained basal activity (Fig. 7, A and C, gray-green). In contrast, single-alanine substitutions at Ser^{1928} or Thr^{1704} had no significant effect on coupling efficiency or Ba^{2+} currents (Fig. 7, A and C, blue and orange). Analyses of the coupling efficiency of individual cells supported these conclusions (fig. S2B). Five of eight (62.5%) cells coexpressing $Ca_V1.2\Delta1800$(T1704A) + DCT with AKAP15 and 5 of 10 (50%) cells coexpressing $Ca_V1.2\Delta1800$ + DCT(S1928A) with AKAP15 showed a higher coupling efficiency in the presence of 5 μM forskolin than the maximum observed with $Ca_V1.2\Delta1800$ + DCT in the absence of forskolin (fig. S2D). In contrast, no individual cells showed a coupling efficiency in the same range when cells coexpressing $Ca_V1.2\Delta1800$(S1700A) + DCT and AKAP15 were treated with 5 μM forskolin. Collectively, these results indicate that

phosphorylation of Ser^{1700} is required for PKA-mediated stimulation of $Ca_V1.2$ channels and that phosphorylation of Thr^{1704} plays a primary role in regulation of basal activity. We did not identify a contribution for phosphorylation of Ser^{1928} to short-term regulation of $Ca_V1.2$ channel activity.

DISCUSSION

Reconstitution of physiological regulation of $Ca_V1.2$ channels in non-muscle cells

PKA-mediated regulation of $Ca_V1.2$ channels in cardiac myocytes has several enigmatic aspects. The C-terminal domain is proteolytically processed in vivo (20,46), but is required for regulation of $Ca_V1.2$ channels in cardiac myocytes (34). Despite the high concentration of PKA, AKAP anchoring is required for β-adrenergic regulation in ventricular myocytes (33); however, the AKAP15 binding site is located in the proteolytically processed distal C-terminal domain (33). This unexpected set of properties has confounded previous attempts to reconstitute PKA-dependent regulation of $Ca_V1.2$ channels in non-muscle cells, as required to define the molecular mechanism of this process. Indeed, only slight PKA-dependent modulation of full-length $Ca_V1.2$ channels has been previously observed, even with coexpression ofAKAP150 [for instance, (31,35,36,42)], raising the possibility that key molecular components of the in vivo $Ca_V1.2$ channel complex were missing from these reconstituted systems. Our results resolve this conundrum. Here, we show that a reconstituted autoinhibitory $Ca_V1.2$ channel signaling complex containing AKAP15 and the noncovalently associated distal C-terminal domain is both necessary and sufficient to reconstitute physiological levels of PKA-dependent regulation of $Ca_V1.2$ channels, and we identify key phosphorylation sites that are required for basal regulation of $Ca_V1.2$ channel activity and for the PKA-dependent increase of channel activity. Because our reconstitution system incorporates all of the previously described characteristics of regulation of cardiac $Ca_V1.2$ channels in vivo, and resolves the apparent paradoxes in the previous in vivo studies, these results provide a conceptual and molecular framework for calcium channel regulation in the fight-or-flight response, in which PKA phosphorylation mediates disinhibition of an autoinhibitory signaling complex containing $Ca_V1.2\Delta1800$ + DCT and AKAP15.

Requirement for AKAP15 for reconstitution of PKA regulation

AKAP15 was identified biochemically in purified preparations of skeletal muscle $Ca_V1.1$ channels (29) and cloned from skeletal and cardiac muscle (30,31), where it was also designated AKAP18 (31). It anchors PKA to both $Ca_V1.1$ and $Ca_V1.2$ channels (29–31), and its interaction with the distal C-terminal domain of $Ca_V1.2$ channels is required for β-adrenergic regulation through the PKA pathway in ventricular myocytes (33). Consistent with this requirement for AKAP in ventricular myocytes, we find that AKAP15 is required for reconstitution of PKA-dependent modulation in non-muscle cells, supporting the conclusion that our in vitro reconstitution mimics this aspect of PKA regulation in vivo.

Requirement for noncovalent association of the distal C-terminal domain for PKA regulation of $Ca_V1.2$ channels

A surprising conclusion from our results is that the distal C-terminal domain is required for $Ca_V1.2$ channel regulation, but is effective only when it is noncovalently associated. Most $Ca_V1.2$ channels in cardiac and skeletal muscle are truncated near the center of the C terminus (18–20,46), and about half of $Ca_V1.2$ channels in neurons are also truncated (23). The distal C-terminal domain is not degraded and is retained in noncovalent association with the channel (21,28). Furthermore, the distal C-terminal domain is required for β-adrenergic regulation of truncated $Ca_V1.2$ channels in cardiac myocytes (34). Therefore, the

requirement for noncovalent association of the distal C-terminal domain observed in our reconstitution system mimics this requirement in cardiac myocytes.

It is unexpected that the distal C-terminal domain is required for anchoring AKAP15 and PKA and yet must be truncated and noncovalently associated to mediate channel regulation. Our biochemical studies provide an explanation for this paradox. When full-length $Ca_V1.2$ channels are studied, activation of PKA does not increase phosphorylation of Ser^{1700} (Fig. 5D). In contrast, activation of PKA increases phosphorylation of Ser^{1700} substantially for $Ca_V1.2\Delta1800$ + DCT (Fig. 5D). Evidently, covalent association of the distal C-terminal in the full-length $Ca_V1.2$ channel occludes Ser^{1700} and reduces or prevents its phosphorylation by PKA. These results support the conclusion that the noncovalently associated complex of $Ca_V1.2$ channels with DCT is the primary physiological substrate for PKA-dependent enhancement of channel activity.

PKA-mediated enhancement of $Ca_V1.2$ channel activity results from disinhibition

The distal C-terminal inhibits the activity of $Ca_V1.2$ channels when it is noncovalently associated (28). Our results show that PKA phosphorylation reverses this inhibition and returns the activity of the noncovalently associated complex of $Ca_V1.2\Delta1800$ + DCT to nearly that observed for $Ca_V1.2\Delta1800$ alone. These results illustrate an additional essential property of the distal C-terminal domain—it must inhibit $Ca_V1.2$ channel activity so that PKA-mediated phosphorylation can relieve that inhibition and increase channel activity. Molecular models suggest that Ser^{1700} and Thr^{1704} are located at the interface between the DCRD and the PCRD, where we have shown that charge-neutralizing mutations can block the inhibitory effects of the DCRD (Fig. 5A) (28). These results predict that phosphorylation at Ser^{1700} and Thr^{1704} would disrupt the interaction between these two domains and lead to disinhibition of the channel. Thus, PKA-dependent regulation of $Ca_V1.2$ channels proceeds through disinhibition of an autoinhibited signaling complex of $Ca_V1.2\Delta1800$, non-covalently associated DCT, and AKAP15. This mode of regulation by dis-inhibition of an autoinhibited signaling complex is unique for ion channels studied to date.

Differential regulation of basal and PKA-dependent $Ca_V1.2$ channel activity by protein phosphorylation

The basal activity of $Ca_V1.2$ channels is decreased by inhibition of PKA and by mutation of Ser^{1700} and Thr^{1704} (Figs. 2 and 6). These results implicate phosphorylation of Ser^{1700} by PKA and Thr^{1704} by casein kinase II in regulation of basal $Ca_V1.2$ channel activity in unstimulated cells. In contrast, the forskolin-dependent increase in $Ca_V1.2$ channel activity required phosphorylation of Ser^{1700}, and little or no contribution of phosphorylation of Thr^{1704} or Ser^{1928} was detected. Because the response to activation of PKA was completely blocked for mutant S1700A, it is likely that Ser^{1700} is the primary site of regulation of $Ca_V1.2$ channels in response to the β-adrenergic receptor–PKA signaling pathway.

In contrast to Ser^{1700} and Thr^{1704} in the proximal C-terminal domain, Ser^{1928} is located far from the interface between the DCRD and the PCRD. Although Ser^{1928} is phosphorylated after β-adrenergic activation in ventricular myocytes (25), we found no effect of Ser^{1928} phosphorylation in regulation of $Ca_V1.2$ channels in our reconstituted regulatory system. In this respect, our results fit closely with those observed in vivo, where phosphorylation of Ser^{1928} was found not to be required for β-adrenergic regulation of $Ca_V1.2$ channels in cardiac myocytes in studies using viral transduction or mouse knock-in mutation methods (34,44). Because Ser^{1928} is robustly phosphorylated in response to β-adrenergic stimulation, it seems likely that its phosphorylation serves an unidentified regulatory function.

Dual regulatory role of the distal C-terminal domain of $Ca_V1.2$ channels

The distal C-terminal domain of $Ca_V1.2$ channels has been implicated in regulation of gene expression in heart (47) and brain (48). In cardiac myocytes, some of the proteolytically cleaved distal C-terminal domain is found in the nucleus and can regulate the transcription of $Ca_V1.2$ messenger RNA (mRNA) (47). In brain neurons, the distal C-terminal domain is proteolytically processed in response to calcium entry (24). The distal C-terminal protein is localized in the nuclei of a small fraction of brain neurons and can regulate the transcription of neuronal genes (48). The distal C-terminal domain also binds the calcium-dependent phosphatase calcineurin through anchoring by AKAP150 (36), and anchored calcineurin dephosphorylates the transcription factor NFAT (nuclear factor of activated T cells) and regulates gene expression (36).

$Ca_V1.2$ channel regulation and disease

Heart failure is one of the most debilitating diseases of the cardiovascular system. Increasing evidence indicates that heart failure involves, at least in part, a maladaptive regulation of calcium signaling in the heart, in which normal β-adrenergic regulation of $Ca_V1.2$ channels fails (49,50). The importance of precise regulation of $Ca_V1.2$ channels is also illustrated by Timothy syndrome, a multifaceted disease in which mutations that impair voltage-dependent inactivation cause arrhythmia, developmental abnormalities, and autism spectrum disorder (51). Our results provide the molecular basis for future investigations of the role of misregulation of $Ca_V1.2$ channels by the PKA pathway in heart failure, Timothy syndrome, and other diseases.

MATERIALS AND METHODS

Antibodies and cDNA constructs

cDNA constructs (28), antibody against $Ca_V1.2$, and antibody against pS^{1928} (20) were described previously. Phosphospecific antibody against $Ca_V1.2$-pS^{1700} was generated against residues ^{1694}EIRRAIpSGDLTAEEEL in the proximal C terminus (Pacific Immunology). Mutants S1700A, T1704A, and S1928A were constructed as described in the Supplementary Materials. GST-$Ca_V1.2$(1670–1731) peptides were expressed and purified from BL21-STAR *Escherichia coli*.

Electrophysiology

tsA-201 cells were transfected, whole-cell voltage clamp recordings were performed, and data were analyzed as previously described (28) (see Supplementary Materials). All data are expressed as means ± SEM of *n* cells. Statistical significance was tested with Student's *t* test for pairwise analysis, and analysis of variance (ANOVA) followed by Dunnett's test for comparison of multiple conditions.

Immunofluorescence, immunoblots, and MS

For immunofluorescence experiments, cells were rinsed with phosphate buffered saline (PBS) (pH 7.4) and fixed for 45 min in 4% paraformaldehyde. Indirect immunofluorescence detection was performed with antibody against $Ca_V1.2$-pS^{1700} and biotinylated goat antibody against rabbit. Samples for all images were prepared identically and viewed at a common gain to permit qualitative comparisons. For immunoblot analysis, cells were washed with PBS 24 hours after transfection and treated with drugs as indicated; membranes were collected, solubilized, and separated by SDS–polyacrylamide gel electrophoresis (SDS-PAGE); and the resulting blots were probed with the indicated antibodies. For MS, phosphorylated GST-$Ca_V1.2$(1670–1731) peptides were digested with trypsin and subjected

to liquid chromatography–MS (LC-MS) analysis. See Supplementary Materials and Methods for details.

Supplementary Material

Refer to Web version on PubMed Central for supplementary material.

Acknowledgments

We thank K. Konoki, E. Sharp, and J. Hulme for technical assistance and cDNA constructs and R. Westenbroek for advice on anti-phosphopeptide antibody design and immunocytochemistry.

Funding: This work was funded by NIH grants R01-HL085372 (to W.A.C.), N01-HV28179 (to W.A.C. and M.A.E.), and T32-HL007312 (to M.D.F. and M.A.E.) and American Heart Association grant 2009POST2080270 (to M.D.F.).

REFERENCES AND NOTES

1. Reuter H. The dependence of slow inward current in Purkinje fibres on the extra-cellular calcium-concentration. J Physiol. 1967; 192:479–492. [PubMed: 6050160]
2. Tsien RW, Giles W, Greengard P. Cyclic AMP mediates the effects of adrenaline on cardiac Purkinje fibres. Nat New Biol. 1972; 240:181–183. [PubMed: 4343950]
3. Tsien RW, Bean BP, Hess P, Lansman JB, Nilius B, Nowycky MC. Mechanisms of calcium channel modulation by β-adrenergic agents and dihydropyridine calcium agonists. J Mol Cell Cardiol. 1986; 18:691–710. [PubMed: 2427730]
4. Osterrieder W, Brum G, Hescheler J, Trautwein W, Flockerzi V, Hofmann F. Injection of subunits of cyclic AMP-dependent protein kinase into cardiac myocytes modulates Ca^{2+} current. Nature. 1982; 298:576–578. [PubMed: 6285199]
5. Bean BP, Nowycky MC, Tsien RW. β-Adrenergic modulation of calcium channels in frog ventricular heart cells. Nature. 1984; 307:371–375. [PubMed: 6320002]
6. Trautwein W, Hescheler J. Regulation of cardiac L-type calcium current by phosphorylation and G proteins. Annu Rev Physiol. 1990; 52:257–274. [PubMed: 2158764]
7. McDonald TF, Pelzer S, Trautwein W, Pelzer DJ. Regulation and modulation of calcium channels in cardiac, skeletal, and smooth muscle cells. Physiol Rev. 1994; 74:365–507. [PubMed: 8171118]
8. Bers DM. Cardiac excitation–contraction coupling. Nature. 2002; 415:198–205. [PubMed: 11805843]
9. Takahashi M, Seagar MJ, Jones JF, Reber BF, Catterall WA. Subunit structure of dihydropyridine-sensitive calcium channels from skeletal muscle. Proc Natl Acad Sci USA. 1987; 84:5478–5482. [PubMed: 2440051]
10. Mikami A, Imoto K, Tanabe T, Niidome T, Mori Y, Takeshima H, Narumiya S, Numa S. Primary structure and functional expression of the cardiac dihydropyridine-sensitive calcium channel. Nature. 1989; 340:230–233. [PubMed: 2474130]
11. Ellis SB, Williams ME, Ways NR, Brenner R, Sharp AH, Leung AT, Campbell KP, McKenna E, Koch WJ, Hui A, Schwartz A, Harpold MM. Sequence and expression of mRNAs encoding the α_1 and α_2 subunits of a DHP-sensitive calcium channel. Science. 1988; 241:1661–1664. [PubMed: 2458626]
12. Ruth P, Röhrkasten A, Biel M, Bosse E, Regulla S, Meyer HE, Flockerzi V, Hofmann F. Primary structure of the β subunit of the DHP-sensitive calcium channel from skeletal muscle. Science. 1989; 245:1115–1118. [PubMed: 2549640]
13. Perez-Reyes E, Castellano A, Kim HS, Bertrand P, Baggstrom E, Lacerda AE, Wei XY, Birnbaumer L. Cloning and expression of a cardiac/brain β subunit of the L-type calcium channel. J Biol Chem. 1992; 267:1792–1797. [PubMed: 1370480]
14. Gao T, Puri TS, Gerhardstein BL, Chien AJ, Green RD, Hosey MM. Identification and subcellular localization of the subunits of L-type calcium channels and adenylyl cyclase in cardiac myocytes. J Biol Chem. 1997; 272:19401–19407. [PubMed: 9235939]

15. Striessnig J. Pharmacology, structure and function of cardiac L-type Ca^{2+} channels. Cell Physiol Biochem. 1999; 9:242–269. [PubMed: 10575201]
16. Richards MW, Butcher AJ, Dolphin AC. Ca^{2+} channel β-subunits: Structural insights AID our understanding. Trends Pharmacol Sci. 2004; 25:626–632. [PubMed: 15530640]
17. Davies A, Hendrich J, Van Minh AT, Wratten J, Douglas L, Dolphin AC. Functional biology of the $\alpha_2\delta$ subunits of voltage-gated calcium channels. Trends Pharmacol Sci. 2007; 28:220–228. [PubMed: 17403543]
18. De Jongh KS, Merrick DK, Catterall WA. Subunits of purified calcium channels: A 212-kDa form of α_1 and partial amino acid sequence of a phosphorylation site of an independent β subunit. Proc Natl Acad Sci USA. 1989; 86:8585–8589. [PubMed: 2554320]
19. De Jongh KS, Warner C, Colvin AA, Catterall WA. Characterization of the two size forms of the α1 subunit of skeletal muscle L-type calcium channels. Proc Natl Acad Sci USA. 1991; 88:10778–10782. [PubMed: 1720551]
20. De Jongh KS, Murphy BJ, Colvin AA, Hell JW, Takahashi M, Catterall WA. Specific phosphorylation of a site in the full-length form of the α1 subunit of the cardiac L-type calcium channel by adenosine 3′,5′-cyclic monophosphate-dependent protein kinase. Biochemistry. 1996; 35:10392–10402. [PubMed: 8756695]
21. Hulme JT, Konoki K, Lin TW, Gritsenko MA, Camp DG II, Bigelow DJ, Catterall WA. Sites of proteolytic processing and noncovalent association of the distal C-terminal domain of $Ca_v1.1$ channels in skeletal muscle. Proc Natl Acad Sci USA. 2005; 102:5274–5279. [PubMed: 15793008]
22. Brawley RM, Hosey MM. Identification of two distinct proteins that are immunologically related to the α_1 subunit of the skeletal muscle dihydropyridine-sensitive calcium channel. J Biol Chem. 1992; 267:18218–18223. [PubMed: 1325462]
23. Hell JW, Yokoyama CT, Wong ST, Warner C, Snutch TP, Catterall WA. Differential phosphorylation of two size forms of the neuronal class C L-type calcium channel α1 subunit. J Biol Chem. 1993; 268:19451–19457. [PubMed: 8396138]
24. Hell JW, Westenbroek RE, Breeze LJ, Wang KK, Chavkin C, Catterall WA. *N*-methyl-D-aspartate receptor-induced proteolytic conversion of postsynaptic class C L-type calcium channels in hippocampal neurons. Proc Natl Acad Sci USA. 1996; 93:3362–3367. [PubMed: 8622942]
25. Hulme JT, Westenbroek RE, Scheuer T, Catterall WA. Phosphorylation of serine 1928 in the distal C-terminal domain of cardiac $Ca_v1.2$ channels during β1-adrenergic regulation. Proc Natl Acad Sci USA. 2006; 103:16574–16579. [PubMed: 17053072]
26. Wei X, Neely A, Lacerda AE, Olcese R, Stefani E, Perez-Reyes E, Birnbaumer L. Modification of Ca^{2+} channel activity by deletions at the carboxyl terminus of the cardiac α_1 subunit. J Biol Chem. 1994; 269:1635–1640. [PubMed: 7507480]
27. Mikala G, Bodi I, Klockner U, Varadi M, Varadi G, Koch SE, Schwartz A. Characterization of auto-regulation of the human cardiac α1 subunit of the L-type calcium channel: Importance of the C-terminus. Mol Cell Biochem. 2003; 250:81–89. [PubMed: 12962146]
28. Hulme JT, Yarov-Yarovoy V, Lin TW, Scheuer T, Catterall WA. Autoinhibitory control of the $Ca_v1.2$ channel by its proteolytically processed distal C-terminal domain. J Physiol. 2006; 576:87–102. [PubMed: 16809371]
29. Gray PC, Tibbs VC, Catterall WA, Murphy BJ. Identification of a 15-kDa cAMP-dependent protein kinase-anchoring protein associated with skeletal muscle L-type calcium channels. J Biol Chem. 1997; 272:6297–6302. [PubMed: 9045648]
30. Gray PC, Johnston BD, Westenbroek RE, Hays LG, Yates JR III, Scheuer T, Catterall WA, Murphy BJ. Primary structure and function of an A kinase anchoring protein associated with calcium channels. Neuron. 1998; 20:1017–1026. [PubMed: 9620705]
31. Fraser IDC, Tavalin SJ, Lester LB, Langeberg LK, Westphal AM, Dean RA, Marrion NV, Scott JD. A novel lipid-anchored A-kinase anchoring protein facilitates cAMP-responsive membrane events. EMBO J. 1998; 17:2261–2272. [PubMed: 9545239]
32. Hulme JT, Ahn M, Hauschka SD, Scheuer T, Catterall WA. A novel leucine zipper targets AKAP15 and cyclic AMP-dependent protein kinase to the C terminus of the skeletal muscle Ca^{2+} channel and modulates its function. J Biol Chem. 2002; 277:4079–4087. [PubMed: 11733497]

33. Hulme JT, Lin TW, Westenbroek RE, Scheuer T, Catterall WA. β-Adrenergic regulation requires direct anchoring of PKA to cardiac $Ca_v1.2$ channels via a leucine zipper interaction with A kinase-anchoring protein 15. Proc Natl Acad Sci USA. 2003; 100:13093–13098. [PubMed: 14569017]
34. Ganesan AN, Maack C, Johns DC, Sidor A, O'Rourke B. β-Adrenergic stimulation of L-type Ca^{2+} channels in cardiac myocytes requires the distal carboxy terminus of α_{1C} but not serine 1928. Circ Res. 2006; 98:e11–e18. [PubMed: 16397147]
35. Gao T, Yatani A, Dell'Acqua ML, Sako H, Green SA, Dascal N, Scott JD, Hosey MM. cAMP-dependent regulation of cardiac L-type Ca^{2+} channels requires membrane targeting of PKA and phosphorylation of channel subunits. Neuron. 1997; 19:185–196. [PubMed: 9247274]
36. Oliveria SF, Dell'Acqua ML, Sather WA. AKAP79/150 anchoring of calcineurin controls neuronal L-type Ca^{2+} channel activity and nuclear signaling. Neuron. 2007; 55:261–275. [PubMed: 17640527]
37. Kameyama M, Hescheler J, Hofmann F, Trautwein W. Modulation of Ca current during the phosphorylation cycle in the guinea pig heart. Pflugers Arch. 1986; 407:123–128. [PubMed: 2428003]
38. duBell WH, Rogers TB. Protein phosphatase 1 and an opposing protein kinase regulate steady-state L-type Ca^{2+} current in mouse cardiac myocytes. J Physiol. 2004; 556:79–93. [PubMed: 14742732]
39. Davis PD, Elliot LH, Harris W, Hill CH, Hurst SA, Keech E, Kumar MK, Lawton G, Nixon JS, Wilkinson SE. Inhibitors of protein kinase C. 2. Substituted bisindolylmaleimides with improved potency and selectivity. J Med Chem. 1992; 35:994–1001. [PubMed: 1552513]
40. Davies SP, Reddy H, Caivano M, Cohen P. Specificity and mechanism of action of some commonly used protein kinase inhibitors. Biochem J. 2000; 351:95–105. [PubMed: 10998351]
41. McConnachie G, Langeberg LK, Scott JD. AKAP signaling complexes: Getting to the heart of the matter. Trends Mol Med. 2006; 12:317–323. [PubMed: 16809066]
42. Zong X, Schreieck J, Mehrke G, Welling A, Schuster A, Bosse E, Flockerzi V, Hofmann F. On the regulation of the expressed L-type calcium channel by cAMP-dependent phosphorylation. Pflugers Arch. 1995; 430:340–347. [PubMed: 7491257]
43. Mitterdorfer J, Froschmayr M, Grabner M, Moebius FF, Glossmann H, Striessnig J. Identification of PK-A phosphorylation sites in the carboxy terminus of L-type calcium channel α_1 subunits. Biochemistry. 1996; 35:9400–9406. [PubMed: 8755718]
44. Lemke T, Welling A, Christel CJ, Blaich A, Bernhard D, Lenhardt P, Hofmann F, Moosmang S. Unchanged β-adrenergic stimulation of cardiac L-type calcium channels in $Ca_v1.2$ phosphorylation site S1928A mutant mice. J Biol Chem. 2008; 283:34738–34744. [PubMed: 18829456]
45. Emrick M, Sadilek M, Konoki K, Catterall WA. β-Adrenergic-regulated phosphorylation of the skeletal muscle $Ca_V1.1$ channel in the fight-or-flight response. Proc Natl Acad Sci USA. in press.
46. Gerhardstein BL, Gao T, Bunemann M, Puri TS, Adair A, Ma H, Hosey MM. Proteolytic processing of the C terminus of the α_{1C} subunit of L-type calcium channels and the role of a proline-rich domain in membrane tethering of proteolytic fragments. J Biol Chem. 2000; 275:8556–8563. [PubMed: 10722694]
47. Schroder E, Byse M, Satin J. L-type calcium channel C terminus autoregulates transcription. Circ Res. 2009; 104:1373–1381. [PubMed: 19461046]
48. Gomez-Ospina N, Tsuruta F, Barreto-Chang O, Hu L, Dolmetsch R. The C terminus of the L-type voltage-gated calcium channel $Ca_V1.2$ encodes a transcription factor. Cell. 2006; 127:591–606. [PubMed: 17081980]
49. Bodi I, Mikala G, Koch SE, Akhter SA, Schwartz A. The L-type calcium channel in the heart: The beat goes on. J Clin Invest. 2005; 115:3306–3317. [PubMed: 16322774]
50. Marks AR. Heart failure and sudden cardiac death: Causes and cures. Harvey Lect. 2005; 101:39–57. [PubMed: 18030974]
51. Splawski I, Timothy KW, Sharpe LM, Decher N, Kumar P, Bloise R, Napolitano C, Schwartz PJ, Joseph RM, Condouris K, Tager-Flusberg H, Priori SG, Sanguinetti MC, Keating MT. $Ca_v1.2$ calcium channel dysfunction causes a multisystem disorder including arrhythmia and autism. Cell. 2004; 119:19–31. [PubMed: 15454078]

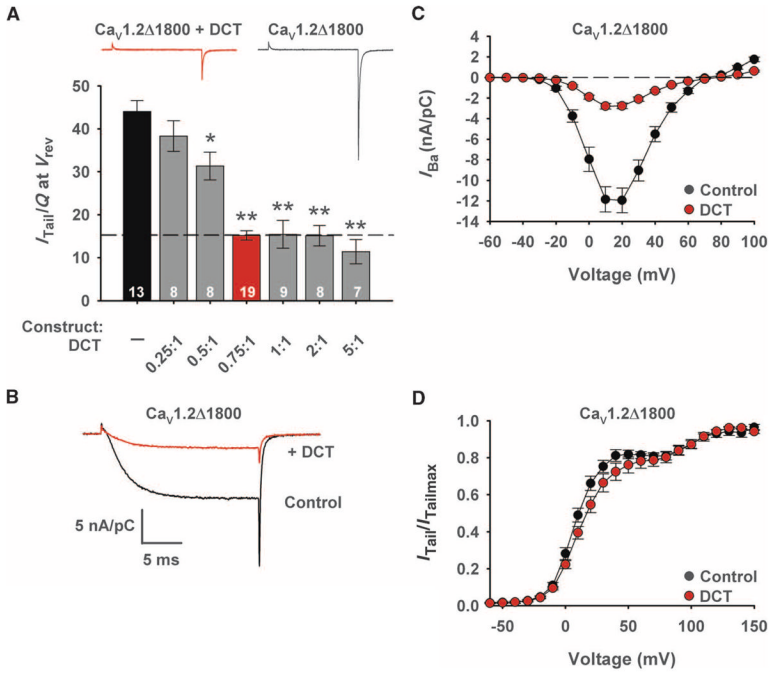

Fig. 1.

Inhibition of $Ca_V1.2\Delta1800$ channels by the distal C terminus. (**A**) Coupling efficiency for $Ca_V1.2\Delta1800$ channels in the presence and absence of the indicated molar ratios of DCT/$Ca_V1.2\Delta1800$ plasmids expressed in tsA-201 cells. *$P < 0.05$ or **$P < 0.01$ versus $Ca_V1.2\Delta1800$ (I_{Tail}, peak tail current; Q, total gating current; V_{rev}, reversal potential). Red symbols indicate 0.75:1 molar ratio. n values and ± SEM are indicated. Significance was determined by ANOVA. Inset: Representative records for $Ca_V1.2\Delta1800$ and $Ca_V1.2\Delta1800$ + DCT channels. (**B**) Representative Ba^{2+} currents through $Ca_V1.2\Delta1800$ and $Ca_V1.2\Delta1800$ + DCT channels elicited by a test pulse to +10 mV from a holding potential of −80 mV. (**C** and **D**) Mean current-voltage (C) and conductance-voltage (D) relationships for $Ca_V1.2\Delta1800$ and $Ca_V1.2\Delta1800$ + DCT channels.

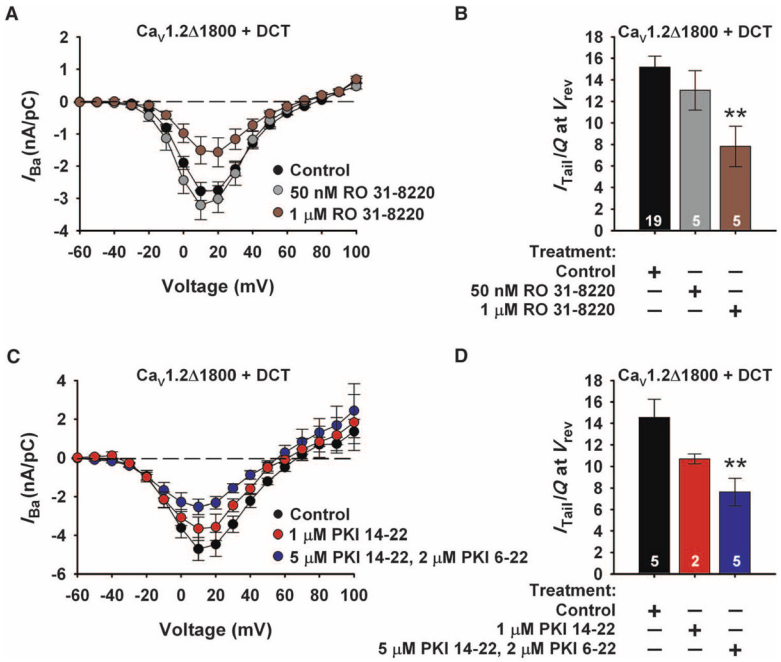

Fig. 2.

Basal activity of $Ca_V1.2$ is reduced by inhibiting kinase activity. (**A**) Current-voltage relationships for $Ca_V1.2\Delta1800$ + DCT in the presence and absence of 50 nM or 1 μM RO 31-8220 (RO). (**B**) Coupling efficiency (nA/pC) for $Ca_V1.2\Delta1800$ + DCT channels in the presence and absence of 50 nM or 1 μM RO 31-8220. $^{**}P < 0.01$. Significance was determined by Student's *t* test (I_{Tail}, peak tail current; *Q*, total gating current; V_{rev}, reversal potential). (**C**) Current-voltage relationships for $Ca_V1.2\Delta1800$ + DCT in the presence and absence of 1 μM myristoylated PKI 14-22 or 5 μM myristoylated PKI 14-22 with 2 μM PKI 6-22. (**D**) Coupling efficiency (nA/pC) for $Ca_V1.2\Delta1800$ + DCT channels in the conditions described in (C). $^{**}P < 0.01$. Significance was determined by Student's *t* test.

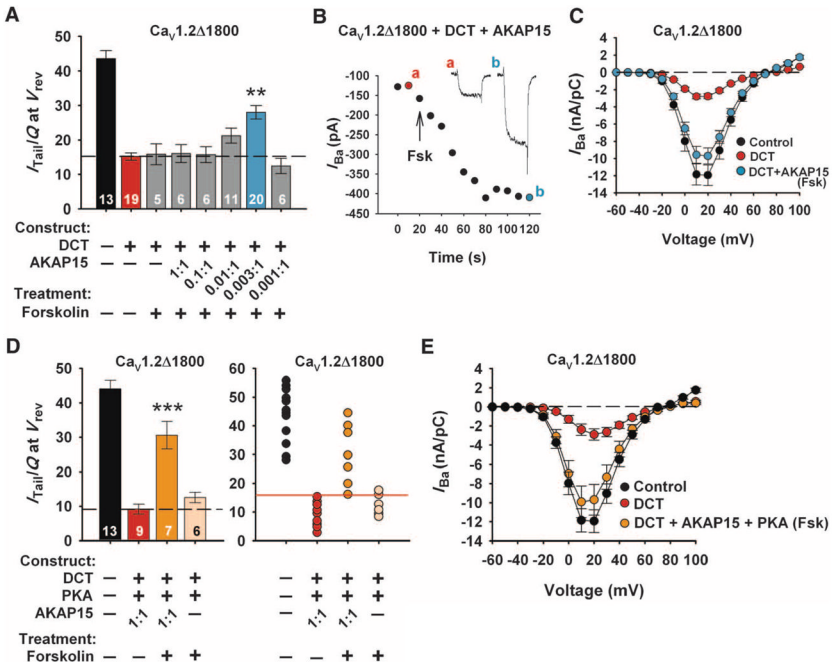

Fig. 3.

Regulation of $Ca_V1.2$ channel activity by optimal expression of cDNA encoding AKAP15. (**A**) Coupling efficiency (nA/pC) for $Ca_V1.2\Delta1800$ and $Ca_V1.2\Delta1800$ + DCT channels with and without AKAP15, and 5 μM forskolin. $^{**}P < 0.01$ versus control without forskolin. Dashed black line indicates mean current for unstimulated $Ca_V1.2\Delta1800$ + DCT (I_{Tail}, peak tail current; Q, total gating current; V_{rev}, reversal potential). (**B**) Time course of peak Ba^{2+} current during perfusion with 5 μM forskolin (Fsk). Pulses to 10 mV before and during application of forskolin. Inset: current traces indicated by a and b. (**C**) Current-voltage relationships of $Ca_V1.2$ channels from (A). (**D**) Coupling efficiency (nA/pC) for $Ca_V1.2\Delta1800$ and $Ca_V1.2\Delta1800$ + DCT channels with PKA Cα catalytic subunit, PKA RIIα regulatory subunit, AKAP15, and 5 μM forskolin. $^{***}P < 0.001$ versus control. Dashed black line indicates mean current for unstimulated $Ca_V1.2\Delta1800$ + DCT. Right, coupling efficiency (nA/pC) of individual experiments in each condition. Red line indicates the maximum current observed with $Ca_V1.2\Delta1800$ + DCT. (**E**) Current-voltage relationships of $Ca_V1.2$ channels from (D). Significance was determined by ANOVA.

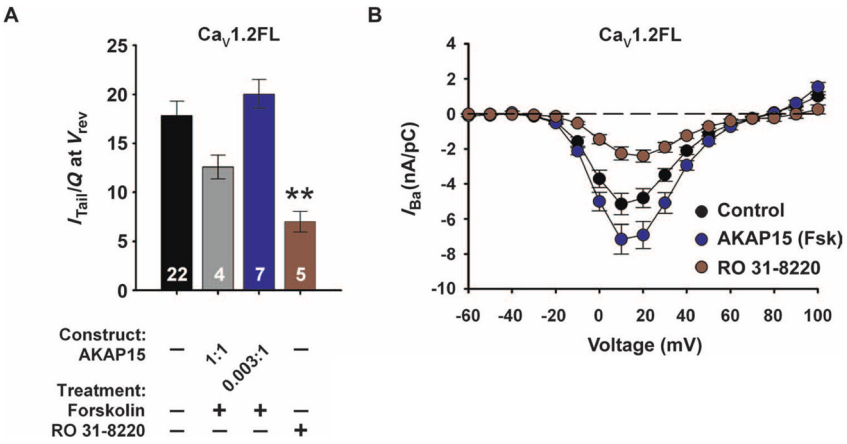

Fig. 4.

Regulation of full-length $Ca_V1.2$ channels. (**A**) Coupling efficiency (nA/pC) for $Ca_V1.2$FL channels in the presence or absence of 1 μM RO 31-8220 or $Ca_V1.2$FL channels with AKAP15 (1:1 or 0.003:1 molar cDNA ratio) and 5 μM forskolin. $^{**}P < 0.01$ (I_{Tail}, peak tail current; Q, total gating current; V_{rev}, reversal potential). (**B**) Current-voltage relationships for the $Ca_V1.2$ channels studied in (A). Significance was determined by Student's *t* test.

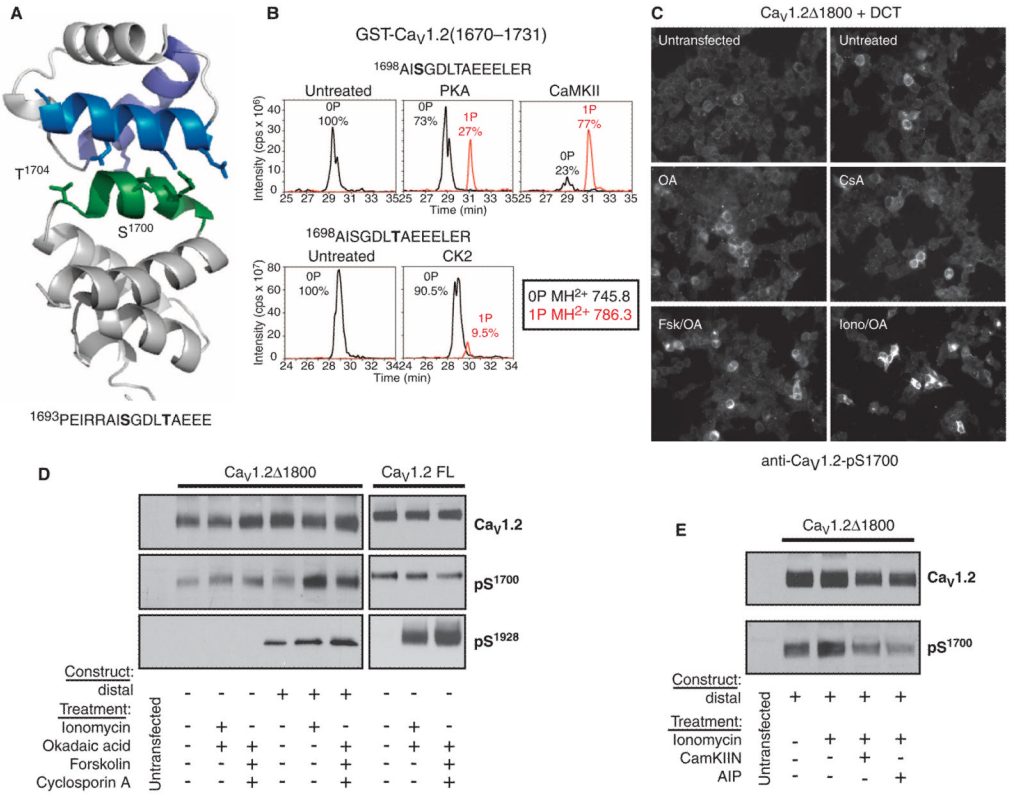

Fig. 5.

Phosphorylation of Ser^{1700} and Ser^{1928} in Ca$_V$1.2 channels. (**A**) Top: docking model of the PCRD-DCRD complex in ribbon representation. Bottom: amino acid sequence surrounding Ser^{1700} and Thr^{1704}. A, Ala; I, Ile; S, Ser; G, Gly; D, Asp; L, Leu; T, Thr; E, Glu; R, Arg. (**B**) Purified GST-Ca$_V$1.2(1670–1731) was phosphorylated with indicated kinases, digested with trypsin, and subjected to LC-MS analysis. MH^{2+} extract ions corresponding to the unphosphorylated (0P) or monophosphorylated (1P) forms of the peptides are indicated. CK2, casein kinase II. (**C**) Cells expressing Ca$_V$1.2Δ1800 + DCT channels were treated as indicated, fixed, probed with antibody against Ca$_V$1.2-pS^{1700}, and visualized by indirect immunofluorescence. OA, okadaic acid; CsA, cyclosporin A; Iono, ionomycin. (**D**) Membranes from cells expressing Ca$_V$1.2FL, Ca$_V$1.2Δ1800, or Ca$_V$1.2Δ1800 + DCT channels were solubilized and separated by SDS-PAGE, and immunoblots were probed with anti-bodies against Ca$_V$1.2, Ca$_V$1.2-pS^{1700}, or Ca$_V$1.2-pS^{1928}. For quantitation, band intensities were normalized to those of the unstimulated control samples (n = 3). (**E**) Cells expressing Ca$_V$1.2Δ1800 + DCT channels, plus cDNA encoding the brain CaMKIIN inhibitor peptide as indicated, were pretreated with ionomycin and autocamtide-2 inhibitory peptide (AIP) and subjected to immunoblot analysis as in (D). For quantitation, band intensities were normalized to those of the unstimulated control samples (n = 3).

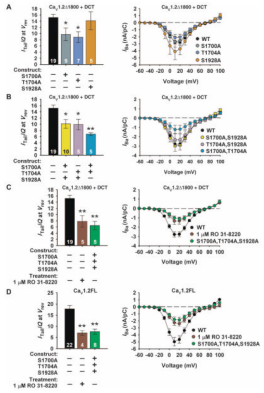

Fig. 6.

Requirements for phosphorylation of Ser[1700], Thr[1704], and Ser[1928] for basal $Ca_V1.2$ channel activity. (**A** and **B**) Coupling efficiency (nA/pC) and current-voltage relationships for wild-type $Ca_V1.2\Delta1800$ + DCT channels or channels with alanine substitutions at Ser[1700], Thr[1704], and Ser[1928] individually or simultaneously. *$P < 0.05$ or **$P < 0.01$ versus wild-type $Ca_V1.2\Delta1800$ + DCT channels (I_{Tail}, peak tail current; Q, total gating current; V_{rev}, reversal potential). (**C**) Coupling efficiency (nA/pC) and current-voltage relationships for $Ca_V1.2\Delta1800$ + DCT channels with triple-alanine substitution (S1700A, T1704A, and S1928A) or wild-type channels in the presence or absence of 1 μM RO 31-8220. **$P < 0.01$ versus $Ca_V1.2\Delta1800$ + DCT channels in control conditions. (**D**) Coupling efficiency (nA/pC) and current-voltage relationships for $Ca_V1.2$FL channels with triple-alanine substitution (S1700A, T1704A, and S1928A) or wild-type channels in the presence or absence of 1 μM RO 31-8220. **$P < 0.01$ versus wild-type $Ca_V1.2$FL channels in control conditions. Significance was determined by ANOVA.

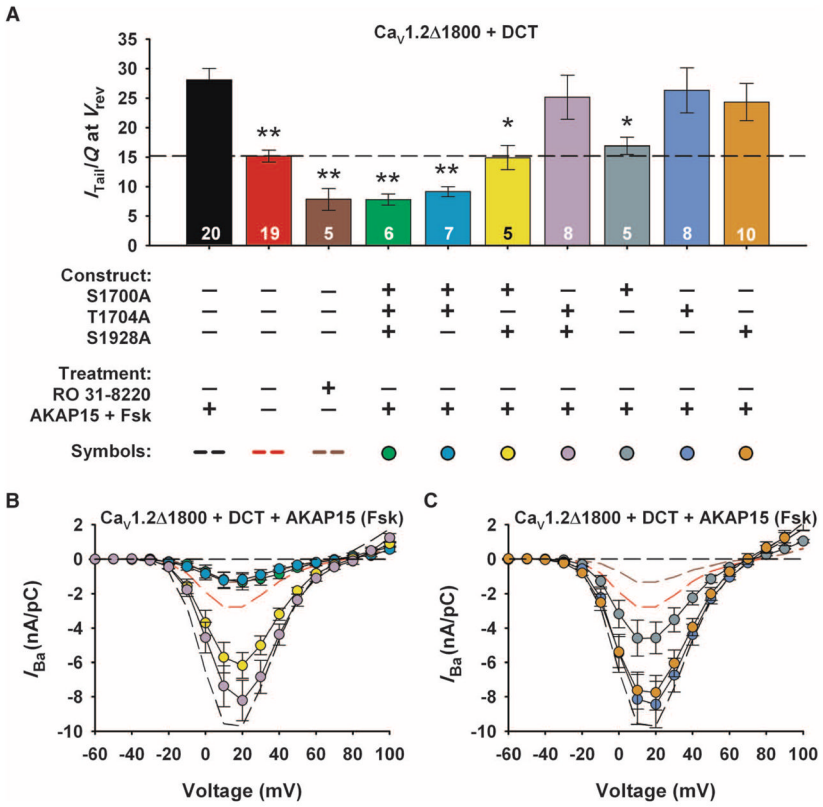

Fig. 7.

Requirement for phosphorylation of Ser^{1700}, Thr^{1704}, and Ser^{1928} for PKA-mediated stimulation of Ca$_V$1.2 channel activity. (**A**) Coupling efficiency for the indicated constructs of Ca$_V$1.2Δ1800 + DCT in the presence or absence of 1 μM RO 31-8220, AKAP15, and 5 μM forskolin. Dashed black line indicates the mean current in unstimulated Ca$_V$1.2Δ1800 + DCT. *P < 0.05 or **P < 0.01 versus AKAP15 and forskolin (I_{Tail}, peak tail current; Q, total gating current; V_{rev}, reversal potential). (**B** and **C**) Current-voltage relationships of Ca$_V$1.2Δ1800 + DCT from (A) as indicated. Significance was determined by ANOVA.